Comparative Analysis of Thermal Performance of a Solar Water Heating System Based on the Serpentine and Risers-Head Configurations

Selfa Johnson Zwalnan[a*], Nanchen Nimyel Caleb[b], Mahan Morgan Mangai[c], Nantim Yohanna Sanda[a]

a Department of Metallurgical Engineering, Plateau State Polytechnic, Barkin-Ladi, Nigeria.
b Department of Computer Engineering, Plateau State Polytechnic, Barkin-Ladi, Nigeria.
c Department of Mechanical Engineering, University of Jos, Plateau State, P. O. Box: 930261, Jos, Nigeria.

ABSTRACT

The effect of solar collector configurations on the thermal efficiency of an active solar water heater was investigated using TRNSYS in this study. Two versions of a solar heater were formulated on the basis of serpentine and riser-header flat plate configurations. Both models were simulated based on the same parameters and weather conditions. Besides, in accordance with clear sky and cloudy sky conditions, a parametric analysis was performed to determine the impact of varying parameters on the thermal efficiency of the two models. The results showed that the serpentine-based device model provided about 2.62 % more usable thermal energy than the riser-header configuration. In addition, both models demonstrated the same response and sensitivity to changes in the collector area and the volume of the tank. However, on a cloudy day, the efficiency of serpentine showed a significant improvement and sensitivity to flow variance with an efficiency gap of about 30 % to the riser header configuration.

1. INTRODUCTION

Solar Water Heaters (SWHs) are used to convert solar energy into heat for both domestic and industrial purposes [1, 2]. This technology eliminates our decade-old dependency on traditional heat sources and thereby, reduces greenhouse gas emissions by reducing electricity consumption for thermal energy requirements [3]. However, due to its original higher cost and lower thermal performance than the traditional energy system, the use of this technology is not widely adopted. Most customers would want to know their monthly saving if they were to convert to solar-powered systems. One major factor influencing the thermal efficiency of the collector is energy loss over time. Interestingly, heat loss in solar collectors is significantly governed by the nature of flow in the collector tubing [4]. On the other hand, the nature of flow and its distributions is a function of the shape and geometry of the collector fluid passage [5]. Minimizing heat loss in the solar collector increases the rate at which the solar energy occurring in the collector transforms into usable thermal energy [6]. Consequently, considerable studies have been conducted to address this problem.

To evaluate the effect of flow rate on the technology and economy of flat plate solar water heating systems, Plaza et al. [4] suggested that a high flow rate would lead to higher solar fractions than a low flow rate. However, the energy consumption of a pump outweighs the gains of using a high flow rate. They, therefore, concluded that a careful search for the proper flow rate to increase the solar fraction and reduce the energy consumption is necessary.

Kim et al. [7] analyzed the thermal performance of the flat plate solar collector based on different shapes of the collector tubing. The goal of their study was to investigate the flow distribution of rectangular, triangular and trapezoidal cross-sections of the collector tubing. Their result revealed that fluid flow in the collector tube with a triangular cross-section was more uniform than the rectangular and trapezoidal sections. Also, in another research, [8, 9] found that the modification of the absorber plate of the primary flat plate collector to a V-groove absorber plate resulted in better thermal performance of the solar collector. Again, they also found that the thermal performance would be better enhanced if the v-groove was made smaller. Jahangiri et al. [10] evaluated the feasibility of the application of solar water heater for space heating and supply of sanitary hot water at 60 °C for a household of 4 persons in 10 provinces of Canada. The study employed the T*Sol simulation software. The findings of the study showed that solar water heater held the potential of reducing the energy demand for hot water in the residential household of Canada by an average of 88.7 % across the ten provinces studied. However, the simulated performance revealed that the system was only capable of supplying an average of 19.18 % of spacing heating demand across the ten studied locations. In a similar study using TSOL, Pahlavan et al. [11] showed that the use of solar water heater in 37 stations in Algeria could

*Corresponding Author's Email: selfajohnspn@gmail.com (S.J. Zwalnan)
URL: http://www.jree.ir/article_122814.html

lead to an annual saving rate of 56783kg/yr of CO_2 in these locations.

Another study by [12] studied the effect of collector arrangement on the thermal performance of a flat plate solar collector. In their conclusion, they agreed that poor collector performance was an indication of an inherently flawed sizing and geometric consideration. Touaba et al. [13] proposed the incorporation of lubricating oil as the absorber plate for a solar water heater integrated with storage tank. Similarly, Hussein et al. [14] enhanced, the thermal performance of a flat plate solar collector using a novel combination of covalent functionalized multi-wall carbon mixed by pure water as the working fluid.

A study to investigate the effect of collector configurations on the thermal performance of the photovoltaic solar thermal energy system was conducted in [9]. In this study, the effect of the collector configuration and the orientation of the building were studied. An extensive review of the various studies conducted in the area of enhancing the thermal performance of solar collectors using nanofluid as working fluid in collectors' tubes was conducted in [15, 16]. In their approach, various properties of the fluid were investigated to determine the sensitivity of the system to change in nanofluid properties. The results of this study showed that molecular structure, hybrid nanofluid content, ingredients, particle shape, temperature, PH value, the concentration of particle volume, and stability of nanofluid had a significant impact on the thermal efficiency of the system. A numerical solution to determining the optimal design parameters of a solar flat plate collector designed to supply hot water was developed in [17]. Matlab software was used to model the time-dependent behavior of the flat plate collector. The sensitivity study shows that the temperature of the heated water and the total coefficient of heat loss decreased with an increase in the water flow rate. The study concluded that the system's flow rate was also a significant indicator of the optimum number of solar collector tubes needed to give the maximum collector outlet water temperatur.Analytical solution to the energy balance of a solar flat plate air heater using the climatic data variables of Jeddah was modeled in [18] to study the thermal performance of a collector. In this study, a computer model of the collector was used to investigate the effect of collector dimension on the collector outlet air temperature. The developed model also investigated the effect of selective coating materials on the solar air heater output temperature. The result showed that the solar air collector coated with nickel-tin outperformed the collector coated with galvanized iron-copper oxide or nickel rhodium black or galvanized iron-cobalt oxide and iron coated with nickel. When comparing the modelled outcome with the measured results, an error of 7.7 % between the modeled output and the experimental performance was also observed. The authors, therefore, concluded that the average annual production of the selectively coated nickel-tin absorber was 29.23 % higher than that of the black painted absorber. In one study, Sachit et al. [19] modeled and simulated the performance of a flat plate solar collector designed to have both the serpentine and the riser-header tube pattern. Also, they compared the performance of the proposed PVT collector with the basic serpentine tube design collector. The result of their findings showed a decrease in the cell temperature with a decrease of about 2 % in the thermal efficiency of the proposed configuration than the serpentine tube pattern configuration. However, a less than 0.04 % improvement to the electrical efficiency of the proposed configuration was observed.

Similarly, different studies have been conducted by many researchers to determine the economics of adopting solar water heating systems for both domestic and industrial applications [10, 20, 21]. In general, a common conclusion is that solar water heating systems have long-term economic and environmental benefits when compared to the conventional energy systems [22-24].

Despite the large volume of research conducted to enhance the thermal performance of the flat plate solar collector, little or no study has provided a side by side thermal assessment of the flat plate collector on an annual basis. Therefore, this research employs a simulation-based approach to evaluate the side by side annual performance of the active solar water heater based on the serpentine and header-riser configurations in the typical tropical climate (Nigeria). The goal here is to assess and compare the influence of collector configuration on the annual thermal output of the heating system in the tropical savannah climate. Additionally, the modeled system was then constructed and tested in order to validate system performance, as predicted by the model. The performance of the system was determined experimentally under the weather and solar condition of Jos, Nigeria.

2. MATERIALS AND METHODS

2.1. System description

The system consists of a flat plate solar collector with a total collector area of 1.5 m^2 which is divided into two sections. In the first section, the collector tubing of the fluid passage is designed based on the risers-header pattern, as shown in Figure 1a. The second section, the fluid channel, is designed in a serpentine pattern, as shown in Figure 1b. Both sections of the collector are distinctively connected to a separate water storage tank of volume 0.03 m^3 (30 litres) through the PVC connecting pipes, thereby creating two independent closed-loop systems. The water in each closed loop is circulated employing a direct current pump powered by a 60 watts solar panel. Notably, the two sections of the collector are covered at the top with a single glass through the entire collector. Consequently, the two sections are identical in all design parameters, as depicted in Table 1. Since water circulation in the system is done through solar pump powered by the solar panel, the natural control ensures that the water is circulated when solar energy falling on the PV module is adequate to produce electrical power. This control is cost-effective and straightforward and eliminates significant costs involved in flow control of solar active water heaters. Figure 2 is the assembled configuration of the proposed solar energy system to be modeled and experimentally evaluated.

2.2. Working principle

When solar radiation from the atmosphere falls on the collector, the absorber plate within the collector is considerably heated to a higher temperature. Consequently, the heat absorbed by the absorber plate is transferred to the circulating fluid (usually water in the direct heating method) flowing through the collector tubing (usually made of copper tubes) attached to the absorber plate. The heated water in the collector returns to the top of the storage tank at a higher temperature. The pump again draws water from the bottom of the tank and pumps it back into the collector, and the entire process is repeated until the sun goes down [25].
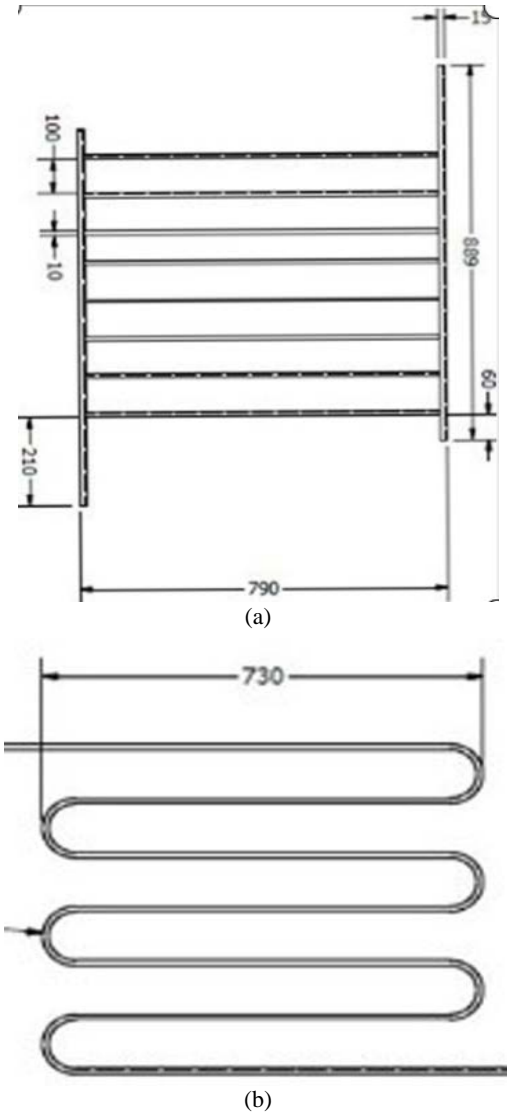
(a)

(b)

Figure 1. Collector tubing of (a) header-riser section of the collector and (b) serpentine section of the collector
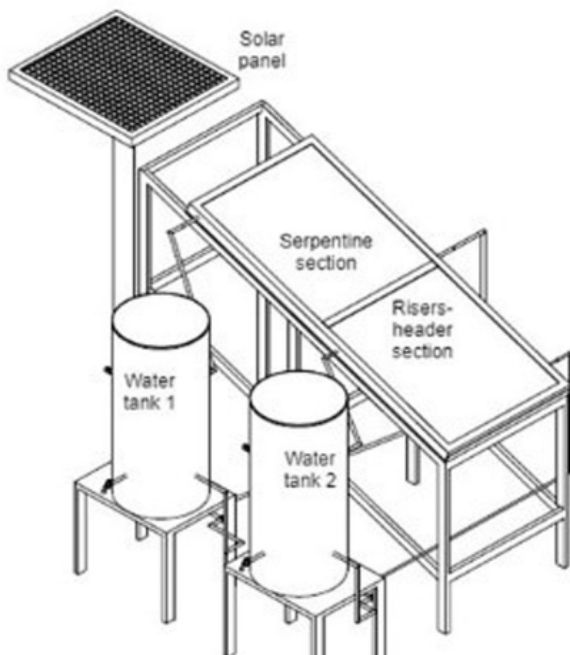

Figure 2. An assembled configuration of the solar water heating system

The process is self-controlled because the pump will continue circulating the water until there is no radiation from the sun. The heated water can be reheated by other forms of conventional heaters when the solar system does not meet up the water temperature requirement.

2.3. The flat-plate energy model

In a steady-state, the Hottel-Whillier-Bliss (HWB) mathematical models and energy balance equations numerically characterize the thermal behavior efficiency of the flat-plate solar collector. At a given moment, the rate of useful energy gain from the solar collector is the positive difference between the energy absorbed by the plate and the energy lost to the atmosphere by the collector, as defined by Eq. (1) [26].

$$\dot{Q}_u = F_R[S - U_L(T_i - T_a)]^+ \tag{1}$$

The plus superscript means that only positive values of the terms are to be used in the square bracket. The absorbed radiation must therefore be greater than the thermal losses, as shown in Figure 3, in order to achieve practical benefits greater than zero.
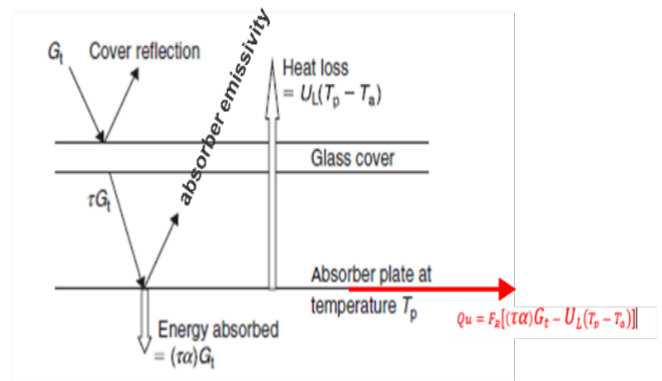

Figure 3. Illustrating the energy balance of a solar collector [27]

In Figure 3, S, U_L, T_i and T_a are the energy absorbed by the absorber plate, the collector overall heat loss coefficient, circulating fluid collector inlet temperature, and the temperature of the surrounding where the collector is placed, respectively. F_R is called the collector heat removal factor. F_R is similar to the heat exchanger effectiveness. For a header-riser flat-plate collector, the collector heat removal factor can be expressed as in Eq.(2) [26]:

$$F_R = \frac{\dot{m}C_p}{A_c U_L}\left[1 - \exp\left(-\frac{A_c U_L F'}{\dot{m}C_p}\right)\right] \tag{2}$$

where F' is the collector efficiency factor expressed as follows:

$$F' = \frac{1/U_L}{W\left[\frac{1}{U_L[D_i+(W-D_i)F]}+\frac{1}{C_b}+\frac{1}{\pi D_i h_{fi}}\right]} \tag{3}$$

F is the standard fin efficiency for straight fins with a rectangular profile, given as:

$$F = \frac{\tanh\left[\frac{m(W-D_i)}{2}\right]}{\frac{m(W-D_i)}{2}} \tag{4}$$

where

$$m = \sqrt{\frac{U_L}{K\delta}} \tag{5}$$

Moreover, U_L is the overall heat loss coefficient for a flat plate collector and it is composed of the top loss coefficient, the edge loss coefficient, and the back loss coefficient. The relation for collector overall heat loss coefficient, U_L, is expressed as:

$$U_L = U_t + U_e + U_b \tag{6}$$

Duffie and Beckman [12] made an approximate reference to the top loss coefficient of the collector as:

$$U_{top} = A + B \tag{7}$$

$$A = \cfrac{1}{\cfrac{N_G}{\frac{C}{T_{pm}}\left[\frac{T_{pm}-T_a}{N_G+f}\right]^e + \frac{1}{h_w}}}$$

$$B = \cfrac{\left[\sigma(T_{pm}{}^2 + T_a{}^2)\right]\left[T_a + T_{pm}\right]}{\cfrac{1}{\varepsilon_p+0.00591N_Gh_w} + \cfrac{2N_G+f-1+0.133\varepsilon_p}{\varepsilon_g} - N_G}$$

where

$$f = (1 + 0.089h_w - 0.1166h_w\varepsilon_p)(1 + 0.07866N_G) \tag{8}$$

$$C = 520[1 - 0.000051\beta^2] \tag{9}$$

$$e = 0.430\left(1 - \frac{100}{T_{pm}}\right) \tag{10}$$

$$h_w = 2.8 + 3V \tag{11}$$

The extent of the conduction loss at the back of the collector is such that the radiation is insignificant. Thus, Duffie and Beckman approximated the back loss, as expressed in Equation (12).

$$U_b = \frac{K_{bi}}{x_{bi}} \tag{12}$$

The edge loss calculated by assuming one-dimensional sideway heat flow around the collector system's perimeter is expressed as:

$$U_e = \frac{K_{ei}}{x_{ei}}\frac{A_e}{A_C} \tag{13}$$

2.4. Evaluation of collector performance indicators

The efficiency matrix of a collector is the parameter that determines how efficiently the collector transforms the total solar energy it absorbs into either thermal energy or electrical energy. The collector efficiency is defined as the ratio of the useful energy from the collector to the total radiation incident on the collector area. This performance matrix of the collector depends on many factors ranging from collector configuration, collector materials and its operating conditions. Theoretically, the thermal efficiency of the Flat Plate Collector (FPC) is expressed as follows:

$$\eta_{coll} = \frac{Q_u}{H_TA_c} = \frac{F_R[H_T(\tau\alpha) - U_L(T_i - T_a)]^+}{H_T} \tag{14}$$

Eq. (15) is essential and useful for the realistic assessment of collector efficiency based on the technical data of manufacturers of commercially obtained solar collectors. However, in this study, the simulated collector efficiency was evaluated through Eq. (14):

$$\eta_{coll} = a_0 - a_1\left(\frac{T_i - T_a}{H_T}\right) - a_2\left(\frac{T_i - T_a}{H_T}\right)^2 \tag{15}$$

where a_0 is the optical efficiency and a_1 and a_2 represent the first- and second-degree heat loss coefficients obtained by the manufacturer during the indoor testing based on the specific tested flow rate. According to Soteris [27], the value of the optical efficiency a_0 and loss coefficient a_1 of good collectors lies within 0.762 and 0.2125, respectively. Under outdoor testing, it is practical to evaluate the collector efficiency based on Eq. (16) which is the ratio of the quantity of heat received from the fluid exiting the collector and the total amount of solar energy received per unit area of collector in the period usually considered as one hour, where V is the volumetric flow rate of the fluid in the collector and Tout and Tin are the measured outlet and inlet temperatures of the collector.

$$\eta_{coll} = \frac{\rho C_p V(T_{out} - T_{in})}{AH_T} \tag{16}$$

2.5. System design and simulation

For the design of the systems, a simulation-based approach using TRNSYS software was adopted. In the TRNSYS simulation studio, two models of solar water heating systems have been built (see Figure 4). A serpentine, flat plate collector was used as the heating unit in the first model, while the second version used a riser-header flat solar collector as the heating unit. All other system design parameters and dimensions are the same for both systems, as seen in Table 1. Figure 4 shows the monthly average daily solar and ambient condition of Jos Nigeria (latitude 9.8965° N, Longitude 8.8583° E) under which the modeled systems have been simulated and evaluated. Figure 5 is a schematic of the models of the two systems developed in the TRNSYS simulation studio. The system model was used to simulate and assess the annual performance of the system. From Figure 4, the months of June to August had a lower level of solar radiation. This finding was not unexpected as these months correspond to a period with a high amount of rainfall. Therefore, the sky is mostly covered with heavy cloud.
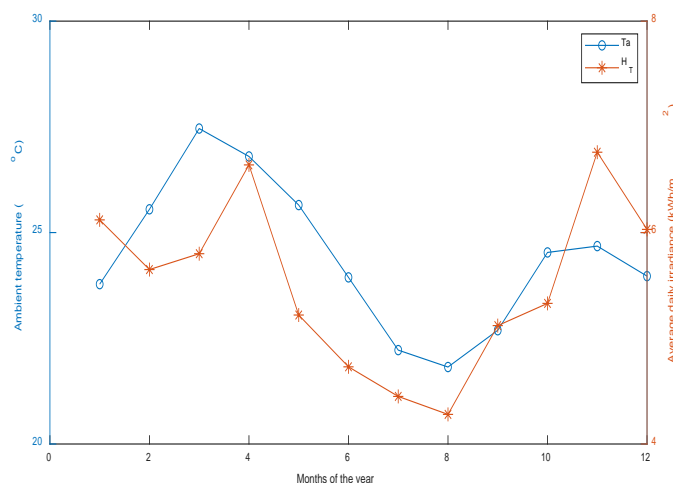

Figure 4. Monthly average daily solar irradiance and ambient temperature of Jos, Nigeria
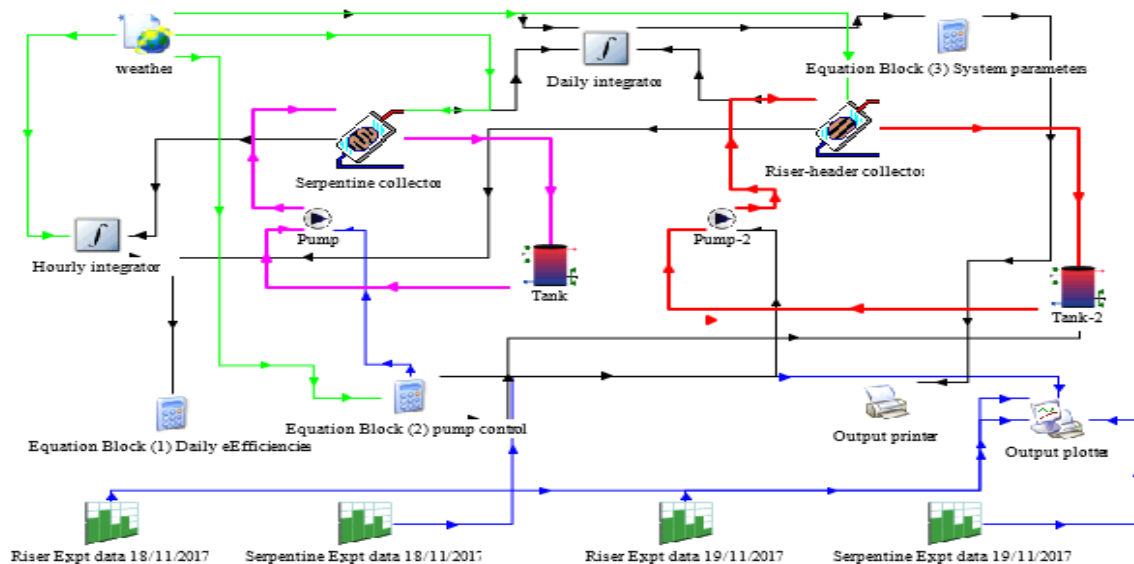
Figure 5. TRNSYS model of the solar water heating system based on the riser-header and serpentine collector configurations

The components of the systems model developed are selected from the TRNSYS simulation studio library. Afterwards, each component is assigned parameters as defined in Table 1. Besides, the output of each component that serves as inputs is transmitted through the connectors to other components.

Interestingly, some components usually have inputs for control. With this control input, the designers can decide how and when this component should operate. A summary of the components and their use and function in this modeling is presented in Table 2 below.

Table 1. System parameters and characteristics

No.	Parameters	Serpentine flat plate	Riser flat plate	Unit
1	Collector length	1.0	1.0	m
2	Collector width	0.8	0.8	m
3	Absorber plate thickness	5	5	mm
4	Conductivity of absorber material	243	243	W/m.K
5	Number of serpentine bends/Number of risers	8	8	-
6	Tube spacing	8	8	cm
7	Serpentine/riser length	0.75	0.75	m
8	Inner tube diameter	1.5	1.5	cm
9	Outer tube diameter	2.0	2.0	cm
10	Fluid specific heat	4.190	4.190	kJ/kg.K
11	Absorptance of the absorber plate	0.94	0.94	Fraction
12	Emissivity of the absorber plate	0.15	0.1'5	Fraction
13	Number of identical covers	1	1	-
14	Index of refraction of cover	1.526	1.526	-
15	Collector tilt	17	17	Degrees
16	Pump rated flow	72	72	Kg/hr.m^2

Source: Author design parameters

Table 2. Summary of the components used in the simulation

Name in studio	Type No. in library	Function
Weather	Type 15	Serving as a function of processing the weather data of a location from an external weather data file at a given time step and making it accessible to other TRNSYS components.
Serpentine collector	Type 565	This component is a model flat solar plate collector where the tube winds up the collector absorber plate in a serpentine fashion.
Riser-header collector	Type 564	This component is a model flat solar plate collector where the tube connects to the collector absorber plate in a riser-header fashion.
Tank 1&2	Type 534	This subroutine models a fluid-filled, constant volume storage tank.
Riser/serpentine Exptl data	Type 14	Type-14 is entirely general; this component can be used to output a set of numbers that fits an individual purpose. The output is dimensionless.
Equation blocks	Not in the library	This component is a means to write scripts that evaluate the entire system performance or control entire or specific component or to parameterize the model.
plotters and printers	Type 65 and 25	The plotter enables visualization of the system performance, while the printer saves the results into an external file.
Integrator	Type 24	It is a utility component used to process the output of simulation by integration of the output in a specific period.

2.6. Parametric analysis

The TRNedit (a TRNSYS engine that enables parametric studies) was employed to conduct parametric analysis in order to understand the sensitivity of the two solar collector models to changes in conditions and parameters. As a result, the three input parameters, namely the collector flowrate, collector area, and tank capacity, are considered as variables in the TRNSYS model. Consequently, a new input file called the deck file is generated and the TRNedit is now executed to simulate the system based on a range of parameters, as shown in Table 3. The results obtained are discussed in Section 3 in this paper. The parametric study is conducted under two weather conditions in order to understand the importance of the volume and quality of solar radiation in the thermal operation of the system. Therefore, the analysis of the parameters was carried out on the basis of the day with a sunny sky and high radiation and the cloudy day with low solar radiation.

Table 3. Range of parameters for system parametric studies

No.	Collector area (m²)	Volume of tank (m³)	v flow rate (kg/hr)
1	0.7	0.03	50.00
2	0.8	0.04	70.00
3	0.9	0.05	90.00
4	1.0	0.06	110.00
5	1.1	0.07	130.00
6	1.2	0.08	150.00
7	1.3	0.09	170.00
8	1.4	0.10	200.00

Source: Author

2.7. Description of the experimental setup and procedure

To compare the simulated performance of the system with that of the experimental system, the solar heater was constructed (see Figure 6) based on the simulated parameters shown in Table 1. The constructed solar water heating system was installed at the Plateau State Polytechnic Clinic, and the outdoor thermal performance of the systems was experimentally measured. The K-type digital thermocouple with a temperature range of -10 °C to 1200 °C ± and 0.04 % uncertainty was mounted at the collector water inlets and outlets of the two systems to measure the outlet and inlet temperatures of the collectors simultaneously at a time interval of 1 hour starting from 8.00 a.m. to 5.00 p.m. for a day in November.

   Within the test period, 0.043 m³ of water was poured into the storage tank before 7.00 a.m. Notably, there is no water drawn from the tank during the experiment to simplify the experimental setup. Furthermore, in each day experiment, the water tank was emptied and charged with fresh water. Moreover, the water circulation pump, which is powered by a solar panel, only runs or circulates water when the solar panel generates enough solar energy. This principle is adopted to circulate the water only when solar energy is available.

2.8. Validation of simulated and predicted performances

The Nash-Sutcliffe Coefficient of Efficiency (NSE) as expressed through Equation (17) [28] was employed to compare the simulated and experimental results so that the simulated model could be validated. The Nash-Sutcliffe Coefficient of Efficiency (NSE) is defined as follows:

$$NSE = 1 - \frac{\sum_{i=1}^{n}(X_{obs,i}-X_{model,i})^2}{\sum_{i=1}^{n}(X_{obs,i}-\overline{X}_{obs})^2} \tag{17}$$

where X_{obs} is the observed value, X_{model} is the modeled value at time/place i., and $\overline{X}_{obs}$ is the mean of the observed values. The value of the NSE ranges from $-\infty$ to 1. The determined NSE value of 1 indicates the exact fit between the model and the experimental values. The closer the NSE value is to 1, the greater the predictive ability of the model used to simulate the actual performance of the system will be.

Figure 6. The developed and installed solar heating experimental setup

3. RESULTS AND DISCUSSION

3.1. Simulated system performance and analysis

The collector inlet temperature significantly affects the collector capacity to convert the absorbed solar energy to useful energy, as seen in Equation (1). Figure 7 shows the simulated variation of inlet temperature from 8.00 a.m to 5.00 p.m for 18th/11/2017 for the modeled collector configurations. According to Figure 7, the temperature behavior of the solar collector slightly differs in terms of the two configurations. The serpentine collector shows greater gain in useful energy evident by the higher inlet temperature than the riser-header collector. This observation is attributed to the collector tubing configuration of the serpentine collector. The spiral patterns of the tubing for the serpentine collector allow the fluid to travel a longer distance in the collector before exiting the collector. Consequently, the heat gain by the fluid is higher for the serpentine than the riser-header collector. According to Figure 6, as the collector inlet temperature increases, the collector efficiency for both the serpentine and the riser header collector decreases. Figure 7 also shows that the collector efficiency of the riser-header collector is slightly lower than that of the serpentine collector. The difference in collector efficiency of the two collectors is not significant, owing to an adequate level of solar radiation on 18/11/2017. However, to ascertain this claim, the parametric analysis of the effect of environmental variables on the collector performance was carried out under two weather scenarios: clear sky and cloudy sky, as presented in the subsequent section.
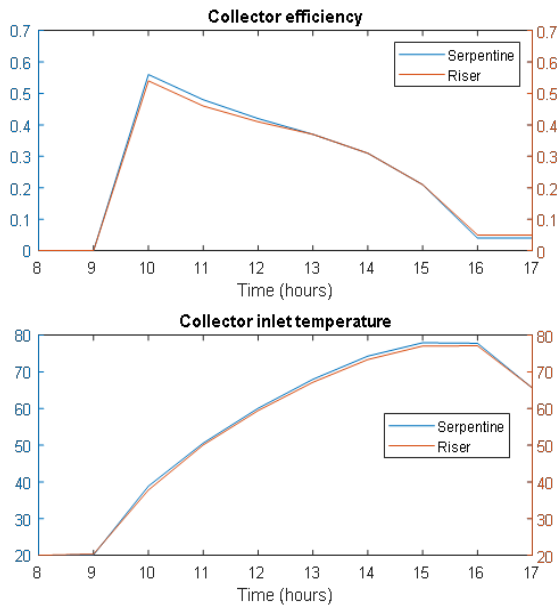
Figure 7. Collector inlet temperature and corresponding efficiency for both serpentine and riser-header collectors

The temperature characteristics of the two configurations, as shown in Figure 6, have not provided significant signs of a big difference between the serpentine and riser-header collector configuration. This assertion supported by the claim of Deng et al. [29] in their findings using Computational Fluid Dynamic (CFD) to calculate the absorber plate temperature of the serpentine and the header-riser configurations of the solar collectors at different collector inlet temperatures. As a result, the analysis of the monthly average daily useful energy of the two collectors is carried out from the simulation result as given in Figure 8. According to this figure, it is clear that the serpentine solar collector has higher useful thermal energy than the header-riser configuration. Concerning the header-riser collector, although Deng et al. [29] showed superior thermal efficiency to the serpentine, the author concluded that the insertion of the flexible silicon tubing in the serpentine tubing was responsible for the reduced efficiency. According to the result of our study and based on the weather condition of the study location (Jos, Nigeria), the annual average useful energy of the serpentine collector was found 2.63 % higher than that of the header-riser collector, as seen in Figure 8. Besides, the monthly analysis of the percentage of the difference in useful energy, as shown in Figure 8b, revealed that the efficacy of the serpentine collector over the riser-header is more significant in months with low solar radiation. This result, therefore, implies that in locations with massive cloud cover, the serpentine collector would strive better than the riser-header collector.

3.2. Collector sensitivity to variance in parameters

For further exploration, the differences in thermal characteristic between the serpentine collector and the riser, header flat plate solar collector, the effect and sensitivity of the two collectors to varying flowrate, tank volume and collector area keeping other condition constants were investigated. Figure 9 shows the response and sensitivity of the two collectors to variance in the collector area while keeping all other parameters constant both for a day with clear sky and a cloudy day. According to Figure 9, for both

collectors, the efficiency of the collector decreases with increase in collector area, while the load and other parameters remain the same. Nonetheless, it is again evident that the serpentine collector shows higher efficiency for both the sunny and cloudy days. Notably, both collectors show the same level of responsiveness to the changes in the collector area as the efficiency line for both collectors exhibits almost the same gradient.
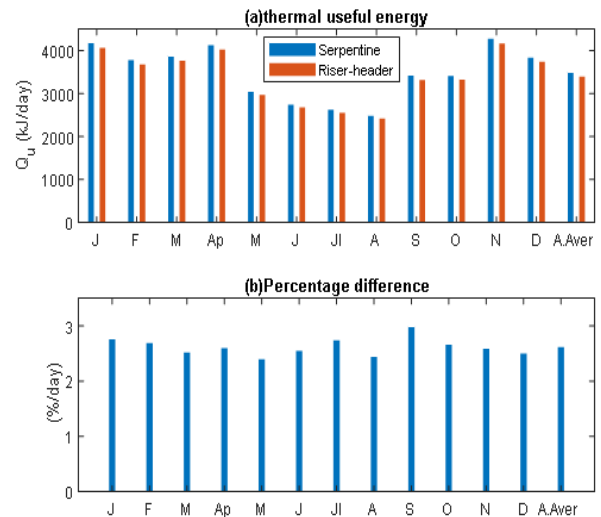

Figure 8. Monthly average daily useful energy and percentage difference in gain of the two collectors
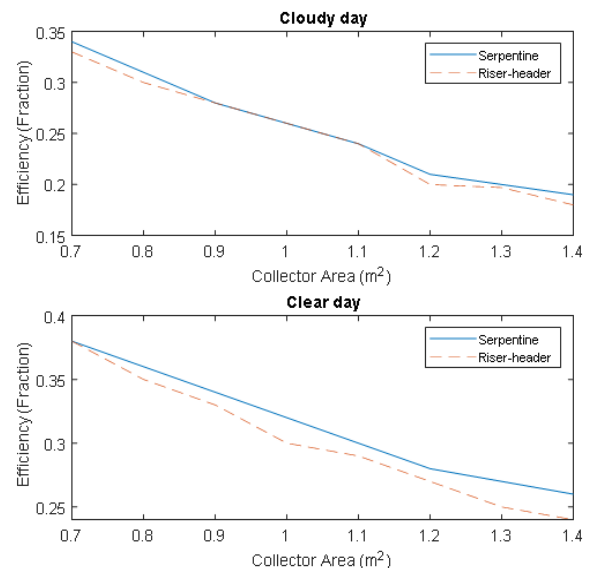

Figure 9. Effect of collector area on the efficiency while keeping other parameters constant

Again, in Figure 10, the graph shows a positive relationship between the collector efficiency and the tank volume. An increase in tank volume is observed to lead to an increase in collector efficiency. However, the serpentine collector still shows higher efficiency than the riser-header collector configuration. Figure 11 shows the variation and sensitivity of the serpentine and the riser-header collector to increase in circulation rate of fluid flow. According to the graph, the riser-header did not show any significant change in the collector efficiency with increasing flow rate for both clear-sky and cloudy sky days.

Interestingly, in Figure 11, the serpentine configuration shows a significant increase in collector efficiency for the flow rate beyond 90 kg/hr on a cloudy day and 170 kg/hr on a clear day. Overall, only the serpentine collector is seen to respond positively to flow rate variations. This observation implies that the serpentine collector configuration response is more sensitive to a change in flow rate, especially with a low level of solar radiation, than the riser-header collector configuration. Therefore, flow rate plays an essential role in increasing the performance of a serpentine collector in a location with a lower solar radiation level than the riser-header configuration.
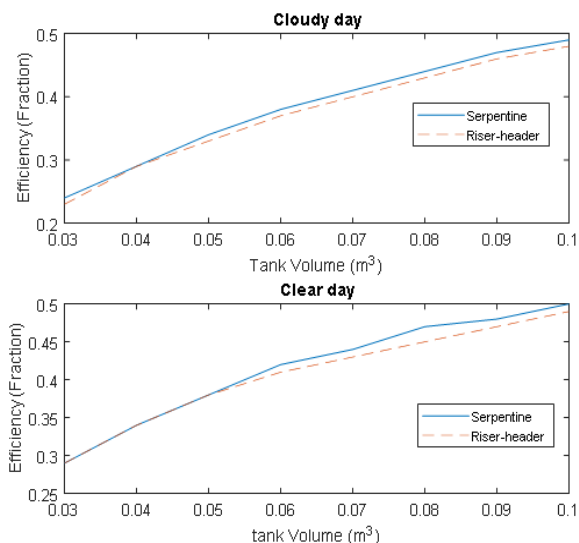

Figure 10. Effect of tank volume on the efficiency while keeping other parameters constant
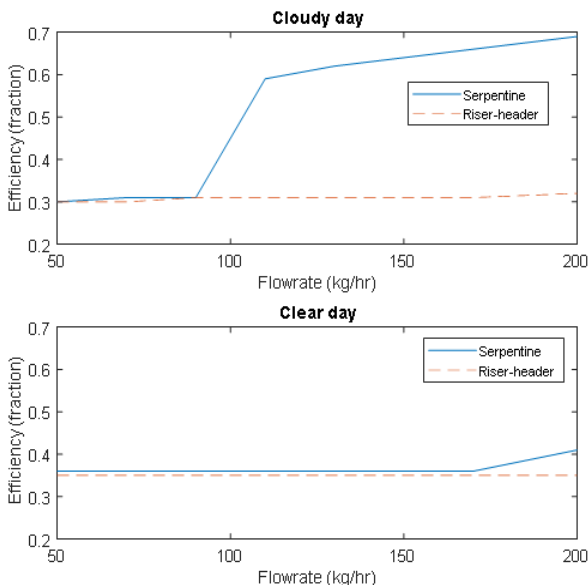

Figure 11. Effect of water flow rate on the efficiency while keeping other parameters constant

3.3. Experimental system performance and model validation

Figure 12 shows the experimental performance of the systems recorded during a test performed on the 18th of November 2017. The thermal behavior of the system shows a very

similar trend in the collector inlet temperature as the simulated performance. The collector inlet was considered for comparison because it is the basis upon which the collector efficiency can be evaluated.
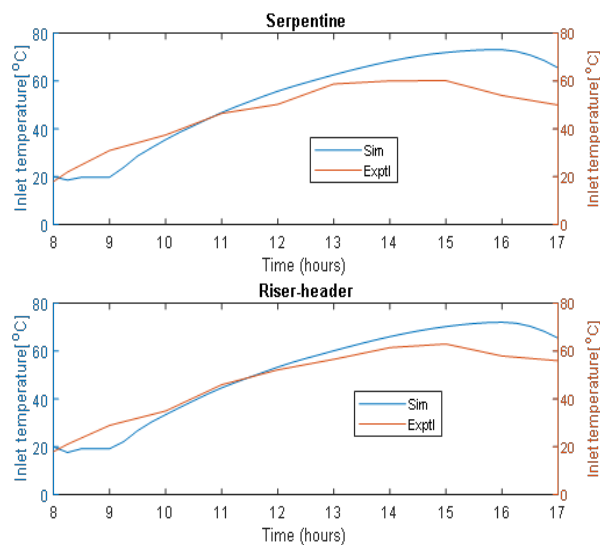

Figure 12. Comparison of the simulated and experimental temperatures of the serpentine and Riser-Header collectors (18th Nov., 2017)

Table 4 shows the calculated NSE between the experimental and simulated performances of the two systems. The experimental performance is in good agreement with the simulated performance with a Nash-Sutcliffe Coefficient of Efficiency (NSE) of 0.82 for both configurations. The Nash-Sutcliffe Coefficient of 0.82 implies that the model predicts the actual performance of the system, with a confidence level of 82 %.

Table 4. NSE between simulated and experimental performances

Collector configuration	NSE
Riser-header	0.82
Serpentine	0.82

4. CONCLUSIONS

The objective of this study is to investigate the effect of solar flat plate configuration on the thermal efficiency of an active solar water heating system. Using TRNSYS software, an active solar water heating system was simulated, and its efficiency was evaluated to achieve this objective. The system was also constructed and tested to validate the predicted performance of the model. The annual thermal output of the serpentine collector from the results obtained was 2.63 % higher than that of the header-riser collector when both collectors operated under the same condition and at a low flow rate of 72 kg/hr. The parametric analysis revealed that both models of the solar heating system demonstrated the same response and sensitivity to variance in the collector area and tank volume. However, the serpentine-based model showed significant improvement and sensitivity to flow variance with an efficiency gap of about 30 % to the riser header configuration on a day with cloudy sky. We, therefore, concluded here that the serpentine model of the solar water heater presented a better choice for locations characterized by highly diffused solar radiation and frequently cloudy sky. The

calculated Nash-Sutcliff coefficient of 0.82 between the modeled inlet temperature of the collector and the measured inlet temperature of the tank on the test day confirmed the validity of the TRNSYS model. The model is, therefore, a fair representation of the complex behavior of the actual system based on the appropriate degree of fit between experimental and simulated results.

5. ACKNOWLEDGEMENT

NOMENCLATURE

F_R	Heat removal factor
$\dot{m}$	Collector fluid mass flow rate (kg/hr.m^2)
C_p	Fluid specific heat (kJ/kg.K)
A_c	Collector area (m^2)
U_L	Overall collector loss coefficient (kJ/m^{2}hr.K)
W	Tube spacing (m)
Cb	Contact resistance (W/m.K)
h_{fi}	Internal fluid heat transfer coefficient (W/m^2.K)
$k\delta$	Plate thermal conductivity and thickness product (kJ/hr.k)
D_i	Internal diameter of the tube (m)
N_G	Number of glass covers
β	Collector tilt (degrees)
ε_g	Emittance of glass
ε_P	Emittance of plate
T_a	Ambient temperature (K)
T_{pm}	Mean plate temperature (K)
h_w	Wind heat transfer coefficient (W/m^2.K)
x_{bi}	Thickness of back material (m)
K_{ei}	Thermal conductivity of edge insulation materials (kJ/hr.m.k)
A_e	Edge insulation area (m^2)
x_{ei}	Insulation thickness at the edge (m)

REFERENCES

1. Gautam, A., Chamoli, S., Kumar, A. and Singh, S., "A review on technical improvements, economic feasibility and world scenario of solar water heating system", *Renewable and Sustainable Energy Reviews*, Vol. 68, (2017), 541-562. (https://doi.org/10.1016/j.rser.2016.09.104).

2. Luo, X., Ma, X., Xu, Y.F., Feng, Z.K., Du, W.P., Wang, R. and Li, M., Solar water heating system, Handbook of energy systems in green buildings, Wang, R. and Zhai, X. Eds., Springer, Berlin, Heidelberg, (2018), 145-194. (https://doi.org/10.1007/978-3-662-49120-1_32).

3. Romero, R.L., Salmerón, L.J.M., Sánchez, R.J., Rodríguez, E.Á. and Álvarez, D.S., "Analysis of the economic feasibility and reduction of a building's energy consumption and emissions when integrating hybrid solar thermal/PV/micro-CHP systems", *Applied Energy*, Vol. 165, (2016), 828-838. (https://doi.org/10.1016/j.apenergy.2015.12.080).

4. Gomariz, F.P., Lopez, J.M.C. and Munoz, F.D., "An analysis of low flow for solar thermal system for water heating", *Solar Energy*, Vol. 179, (2019), 67-73. (https://doi.org/10.1016/jsolener.2018.12.060).

5. Karami, N. and Rahimi, M., "Heat transfer enhancement in a hybrid microchannel-photovoltaic cell using Boehmite nanofluid", *International Communications in Heat and Mass Transfer*, Vol. 55, (2014), 45-52. (https://www.sciencedirect.com/science/article/pii/S0735193314001134).

6. National Renewable Laboratory (NREL), "High performance flat plate solar thermal collector evaluation", (2015), 1-80. (https://www.nrel.gov/docs/fy16osti/66215.pdf).

7. Kim, S., Choi, E. and Cho, Y.I., "The effect of header shapes on the flow distribution in a manifold for electronic packaging applications", *International Communications in Heat and Mass Transfer*, Vol. 22, No. 3, (1995), 329-341. (https://jglobal.jst.go.jp/en/detail?JGLOBAL_ID=200902148672674963).

8. Zulkifle, I., Alwaeli, A.H.A., Ruslan, M.H., Ibarahim, Z., Othman, M.Y.H. and Sopian, K., "Numerical investigation of V-groove air-

9. collector performance with changing cover in Bangi, Malaysia", *Case Studies in Thermal Engineering*, Vol. 12, (2018), 587-599. (https://doi.org/10.1016/j.csite.2018.07.012).

9. Liu, T., Lin, W., Gao, W., Lou, C., Li, M., Zheng, Q. and Xia, C., "A parametric study on the thermal performance of a solar air collector with a V-groove absorber", *International Journal of Green Energy*, Vol. 4, No. 6, (2007), 601-622. (https://www.tandfonline.com/doi/abs/10.1080/15435070701665370).

10. Jahangiri, M., Alidadi Shamsabadi, A. and Saghaei, H., "Comprehensive evaluation of using solar water heater on a household scale in canada", *Journal of Renewable Energy and Environment (JREE)*, Vol. 5, No. 1, (2018), 35-42. (http://dx.doi.org/10.30501/jree.2018.88491).

11. Pahlavan, S., Jahangiri, M., Alidadi Shamsabadi, A. and Khechekhouche, A., "Feasibility study of solar water heaters in Algeria, A review", *Journal of Solar Energy Research*, Vol. 3, No. 3, (2018), 201-211. (https://jser.ut.ac.ir/article_67424.html).

12. Duffie, J.A. and Beckman, W.A., Solar engineering of thermal processes, Fourth edition, New Jersey, John Wiley & Sons Inc., (2013). (https://www.sku.ac.ir/Datafiles/BookLibrary/45/John).

13. Touaba, O., AitCheikh, S., Slimani, M.E., Bouraiou, A. and Ziane, A., "Investigation and prototyping implementation of a novel solar water collector based on used engine oil as HTF", *Proceedings of 4th International Conference on Electrical Engineering and Control Applications (ICEECA)*, *Bououden, S., Chadli, M., Ziani, S. ZI, editor*, (2019) 779-789. (https://www.scopus.com/record/display.uri?eid=2-s2.0-85092711693).

14. Hussein, O.A, Habib, K., Muhsan, A.S., Saidur, R., Alawi, O.A. and Ibrahim, T.K., "Thermal performance enhancement of a flat plate solar collector using hybrid nanofluid", *Solar Energy*, Vol 204, (2020), 208-222. (https://doi.org/10.1016/j.solener.2020.04.034).

15. Raj, P. and Subudhi, S., "A review of studies using nano fl uids in flat-plate and direct absorption solar collectors", *Renewable and Sustainable Energy Review*, Vol. 84, (2018), 54-74. (https://doi.org/10.1016/j.rser.2017.10.012).

16. Kiliç, F., Menlik, ,T. and Sözen, A,. "Effect of titanium dioxide/water nano fluid use on thermal performance of the flat plate solar collector", *Solar Energy*, Vol. 164, (2018), 101-108. (https://doi.org/10.1016/j.solener.2018.02.002).

17. Hamed, M., Fellah, A., Ben, B.A., "Parametric sensitivity studies on the performance of a flat plate solar collector in transient behavior", *Energy Conversion and Management*, Vol. 78, (2014), 938-947. (http://dx.doi.org/10.1016/j.enconman.2013.09.044).

18. El-Sebaii, A.A. and Al-Snani, H., "Effect of selective coating on thermal performance of flat plate solar air heaters", *Energy*, (2010), 1820-1828. (https://doi.org/10.1016/j.energy.2009.12.037).

19. Sachit, F.A., Rosli, M.A.M., Tamaldin, N., Misha ,S. and Abdullah, A.L., "Modelling, validation and analyzing performance of serpentine-direct PV/T solar collector design", *CFD Letter*, Vol. 11, No. 2, (2019), 50-65. (http://www.akademiabaru.com/doc/CFDLV11_N2_P50_65.pdf).

20. Smyth, M.Ã., Eames, P.C. and Norton, B., "Techno-economic appraisal of an integrated collector/storage solar water heater", *Renewable Energy*, Vol. 29, (2004), 1503-1514. (https://doi.org/10.1016/j.renene.2003.10.009).

21. Lang, T., Ammann, D. and Girod, B., "Profitability in absence of subsidies: A techno-economic analysis of rooftop photovoltaic self-consumption in residential and commercial buildings", *Renewable Energy*, Vol. 87, (2016), 77-87. (https://doi.org/10.1016/j.renene.2015.09.059).

22. Koroneos, C.J. and Nanaki, E.A., "Life cycle environmental impact assessment of a solar water heater", *Journal of Cleaner Production*, Vol. 37, (2012), 154-161. (https://doi.org/10.1016/j.jclepro.2012.07.001).

23. Abdon, A., Zhang, X., Parra, D., Patel, M.K., Bauer, C. and Worlitschek, J., "Techno-economic and environmental assessment of stationary electricity storage technologies for different time scales", *Energy*, Vol. 139, (2017), 1173-1187. (https://doi.org/10.1016/j.energy.2017.07.097).

24. Hussain, S. and Harrison, S.J., "Evaluation of thermal characteristics of a flat plate solar collector with a back mounted air channel", *Applied Thermal Engineering*, Vol. 123, (2017), 940-952. (https://doi.org/10.1016/j.applthermaleng.2017.05.121).

25. Soteris, A.K. and Christos, P., "Modelling of a thermosyphon solar water heating system and simple model", *Renewable Energy*, Vol. 21, (2000), 471-493. (https://doi.org/10.1016/S0960-1481(00)00086-0).

26. Diez, F.J., Navas-Gracia, L.M., Martínez-Rodríguez, A., Correa-Guimaraes, A. and Chico-Santamarta, L., "Modelling of a flat-plate solar collector using artificial neural networks for different working fluid (water) flow rates", *Solar Energy*, Vol. 188, (2019), 1320-1331. (https://doi.org/10.1016/j.solener.2019.07.022).

27. Kalogirou, S.A., Designing and modeling solar energy systems, Solar energy engineering, 2nd edition, Oxford OX5 1GB, UK, Academic Press publications, (2014), 583-689. (https://www.elsevier.com/books/solar-energy-engineering/kalogirou/978-0-12-397270-5).

28. Julien, G. A., Emmanuel, L., Clément, A., Rufin, O. A. and Brice A.S., "Modeling solar energy transfer through roof material in Africa Sub-Saharan Regions", *Renewable Energy*, Vol. 34, (2013), 1-8. (https://doi.org/10.1155/2013/480137).

29. Deng, J., O'Donovan, T.S., Tian, Z., King, J. and Speake, S., "Thermal performance predictions and tests of a novel type of flat plate solar thermal collectors by integrating with a freeze tolerance solution", *Energy Conversion and Management*, Vol. 198, (2019), 111784. (https://doi.org/10.1016/j.enconman.2019.111784).